

Synthesis and in Vitro Evaluation of BBB Permeability, Tumor Cell Uptake, and Cytotoxicity of a Series of Carboranylporphyrin Conjugates

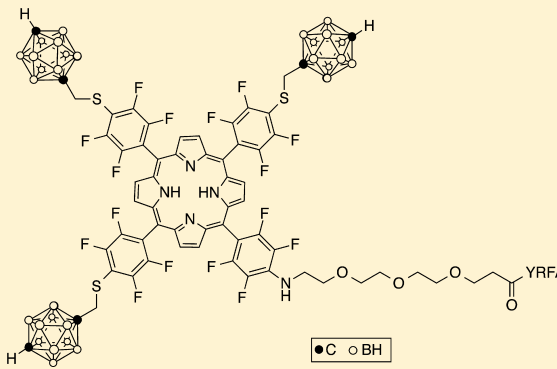
N. V. S. Dinesh K. Bhupathiraju,[†] Xiaoke Hu,[†] Zehua Zhou,[†] Frank R. Fronczek,[†] Pierre-Olivier Couraud,[‡] Ignacio A. Romero,[‡] Babette Weksler,[‡] and M. Graça H. Vicente*,[†]

[†]Department of Chemistry, Louisiana State University, Baton Rouge, Louisiana 70803, United States

[‡]Institut COCHIN, INSERM U1016, CNRS UMR 8104, Université Paris Descartes, 75014 Paris, France

Supporting Information

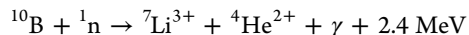
ABSTRACT: A series of tri[(*p*-carboranyl methylthio)-tetrafluorophenyl]porphyrin conjugates of linear and branched polyamines, glucose, arginine, tri(ethylene glycol), and Tyr-D-Arg-Phe- β -Ala (YRFA) peptide were synthesized. These conjugates were investigated for their BBB permeability in human hCMEC/D3 brain endothelial cells, and their cytotoxicity and uptake were assessed using human glioma T98G cells. For comparison purposes, a symmetric tetra[(*p*-carboranyl methylthio)-tetrafluorophenyl]porphyrin was also synthesized, and its crystal structure was obtained. All porphyrin conjugates show low dark cytotoxicity ($IC_{50} > 400 \mu\text{M}$) and low phototoxicity ($IC_{50} > 100 \mu\text{M}$ at 1.5 J/cm^2) toward T98G cells. All conjugates were efficiently taken up by T98G cells, particularly the cationic polyamine and arginine conjugates, and were localized in multiple cellular organelles, including mitochondria and lysosomes. All compounds showed relatively low in vitro BBB permeability compared with that of lucifer yellow because of their higher molecular weight, hydrophobicity, and tendency for aggregation in solution. Within this series, the branched polyamine and YRFA conjugates showed the highest permeability coefficient, whereas the glucose conjugate showed the lowest permeability coefficient.



All compounds showed relatively low in vitro BBB permeability compared with that of lucifer yellow because of their higher molecular weight, hydrophobicity, and tendency for aggregation in solution. Within this series, the branched polyamine and YRFA conjugates showed the highest permeability coefficient, whereas the glucose conjugate showed the lowest permeability coefficient.

INTRODUCTION

Boron neutron capture therapy (BNCT) is a binary treatment methodology for brain tumors and other cancers that involves the irradiation of ^{10}B -containing tumors with low-energy thermal or epithermal neutrons.^{1–3} The nuclear reaction produces excited ^{11}B nuclei, which spontaneously fission to give cytotoxic high linear energy transfer (high-LET) alpha and lithium-7 particles, γ radiation, and about 2.4 MeV of kinetic energy, as shown by the following equation:

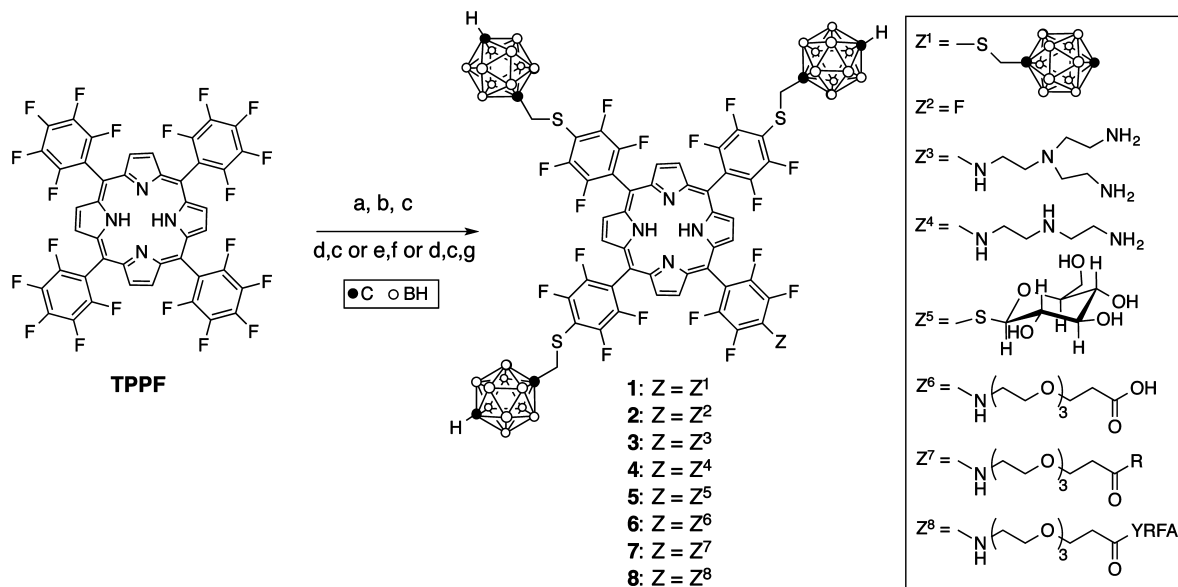


The high-LET particles have relatively short path lengths in tissues of about one cell diameter, limiting the destructive effect to ^{10}B -containing malignant cells. Therefore, BNCT can potentially destroy tumor cells dispersed in normal brain tissue if sufficient amounts of ^{10}B ($\sim 20 \mu\text{g/g}$ weight or $\sim 10^9$ atoms/cell) and low-energy neutrons are selectively delivered. Boron-10 is a nonradioactive isotope with 20% natural abundance that can be incorporated into BNCT agents at the 95–96% level from ^{10}B -enriched starting materials. Effective boron-delivery agents must show low systemic toxicity, deliver therapeutic amounts of boron to target tumors with high (>5) tumor-to-brain and tumor-to-blood concentration ratios, and clear rapidly from normal tissues while persisting in the tumor

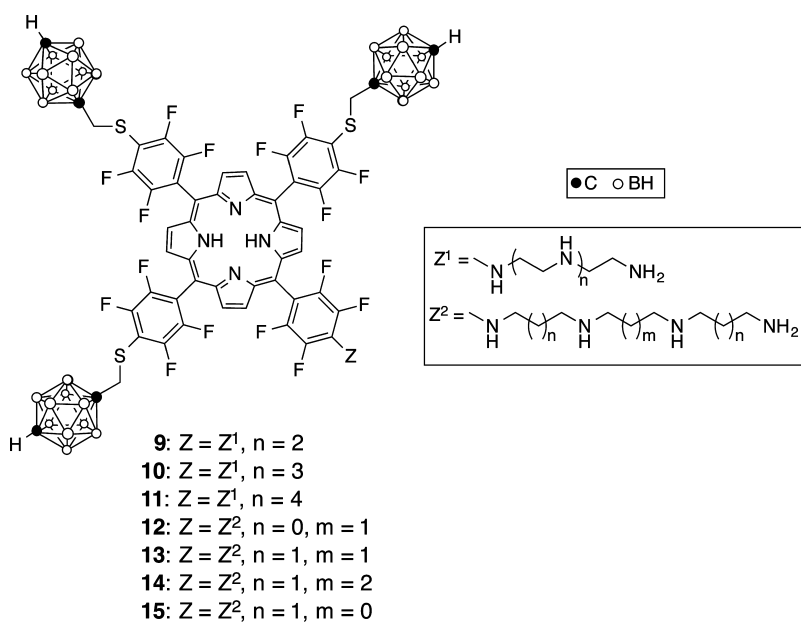
during BNCT. Two BNCT drugs have been used clinically, the sodium salt of the sulfhydryl boron hydride $\text{Na}_2\text{B}_{12}\text{H}_{11}\text{SH}$, known as BSH, and L-4-dihydroxy-borylphenylalanine known as BPA, either alone or in combination for the treatment of high-grade gliomas and recurrent head and neck cancers.^{4–6} Although BSH and BPA have shown to be safe and efficacious in BNCT clinical trials, improved boron-delivery agents of low toxicity and with the ability to deliver high amounts of boron into tumor cells have been the focus of research in recent decades.^{7,8} Among these, boron-containing porphyrins are particularly promising because of their demonstrated high tumor cell uptake and retention, ability to deliver therapeutic amounts of boron intracellularly, and fluorescence and photosensitizing properties, which facilitate the quantification of tissue-localized boron and the possibility of using photodynamic therapy (PDT) as an adjuvant treatment for BNCT.^{9,10} PDT combines a photosensitizer, light, and oxygen to generate reactive oxygen species, including singlet oxygen, that are highly cytotoxic to tissues.^{11,12} Two porphyrin-based macrocycles are FDA-approved as PDT photosensitizers, and several others are under investigation for the PDT treatment of

Received: May 20, 2014

Published: July 16, 2014

Scheme 1^a

^aConditions: (a) mercaptomethyl-*p*-carborane, K₂CO₃, DMF, rt, 48 h (89% for 1); (b) Zn(OAc)₂, methanol/CH₂Cl₂, rt; (c) TFA/chloroform 1:1, rt, 4 h (combined 3 steps, 30% for 2); (d) H₂N-(Boc)-polyamine or H₂N-(CH₂CH₂O)₃CH₂CH₂CO₂'Bu, NMP, 100 °C, 4 h, (95–96%); (e) 1-thiol- β -D-glucose tetraacetate, K₂CO₃, DMF, rt, 48 h (95%); (f) NaOMe, methanol/chloroform, rt, 2 h (93%); (g) L-arginine or YRFA on solid support, HATU, DIEA, DMF, rt. (65–89%).

Figure 1. Porphyrin-polyamine conjugates¹⁷ evaluated in the in vitro BBB model permeability studies.

various malignant and nonmalignant conditions in dermatology, cardiology, and ophthalmology.¹³ The combination of BNCT and PDT is particularly attractive for the treatment of high-grade gliomas and melanomas because it targets different mechanisms of tumor cell destruction and increases the overall therapeutic effect. We have reported the synthesis and investigation of promising dual sensitizers for application in combined PDT and BNCT treatment, H₂TCP^{14,15} and TPFC,¹⁶ that show efficient photosensitizing activity against melanotic melanomas. We have also demonstrated that conjugation of a boron-containing porphyrin to polyamines (Figure 1)¹⁷ or to a cell-penetrating peptide sequence¹⁸ significantly increases their cellular uptake by approximately

12-fold. Herein, we report the synthesis and conjugation of a fluorinated *p*-carbonylmethylthioporphyrin to linear and branched polyamines, glucose, arginine, and Tyr-D-Arg-Phe- β -Ala (YRFA) peptide. Fluorinated porphyrins have been shown to have increased biological efficacy compared with that of their nonfluorinated analogues,^{19–21} and they also allow visualization and quantification of tissue-localized drug via ¹⁸F-PET imaging.²² The conjugation of polyamines to porphyrins has been shown to lead to increased tumor cell uptake as a result of an upregulated polyamine transport system and/or the interaction of the cationic ammonium groups with plasma membrane phosphates.^{17,23–25} Similarly, porphyrins containing one or more arginine groups have demonstrated enhanced

cellular uptake due, in part, to the planar geometry and charge delocalization of the guanidinium group which is uniquely suited for interaction with plasma membrane phosphates.^{26,27} The conjugation of carbohydrates to porphyrin derivatives is another attractive strategy for increasing the solubility and cellular uptake of photosensitizers due to the targeting of carbohydrate-binding lectins highly expressed in tumor cells.^{28–30} Among these, glucose derivatives are particularly promising due to the overexpression of glucose transporters (GLUT)³¹ in tumor cells and in the brain capillary endothelial cells that form the blood–brain barrier (BBB).³² The BBB largely restricts the movement of hydrophilic, high molecular weight molecules between the blood and the brain interstitial fluid, and this constitutes a major challenge for boron delivery in BNCT of brain tumors.^{7–10,32,33} A variety of transporters and receptors are expressed at the BBB for the transport of nutrients and metabolites into the brain, including GLUT1, GLUT3, and μ -opioid receptors. Opioid peptides, including dermorphin and its derivatives such as Tyr-D-Arg-Phe- β -Ala (YRFA), have high affinity for μ -opioid receptors and can cross the BBB via adsorptive-mediated endocytosis.^{34–36} Therefore, the conjugation of a boron-containing porphyrin to polyamines, glucose, arginine and the opioid peptide YRFA could lead to increased BBB permeability and tumor cell uptake for efficient intracellular boron delivery. In this article, we report the synthesis and investigation of a series of conjugates to a fluorinated carboranylporphyrin in human glioma T98G and hCMEC/D3 cells, and we compare their cytotoxicity and ability to cross the BBB and to localize within tumor cells.

EXPERIMENTAL SECTION

Chemistry. Commercially available reagents and solvents (HPLC grade) were purchased from Sigma-Aldrich or Acros Organics and used without further purification. *para*-Carborane was purchased from Katchem, Inc. Anhydrous methanol was prepared by distillation from magnesium and stored under nitrogen over 3 Å molecular sieves. Anhydrous THF was prepared by distillation from sodium and benzophenone. Analytical thin-layer chromatography (TLC) was performed on polyester-backed TLC plates 254 (precoated, 200 μ m, Sorbent Technologies), and silica gel 60 (70–230 mesh, Merk) was used for column chromatography. ¹H and ¹³C NMR spectra were obtained using a Bruker AV-4 400 MHz spectrometer, and ¹⁹F NMR, on a Bruker DPX-250 250 MHz spectrometer; chemical shifts are expressed in ppm relative to CDCl₃ (7.26 ppm, ¹H; 77.0 ppm, ¹³C), (CD₃)₂CO (2.05 ppm, ¹H; 29.84 and 206.26 ppm, ¹³C). Electronic absorption spectra were measured on a PerkinElmer Lambda 35 UV-vis spectrophotometer. Mass analyses were conducted at the LSU Mass Spectrometry Facility on a Bruker Omniplex MALDI-TOF mass spectrometer or on an Applied Biosystems QSTAR XL (for HRMS-ESI). Melting points were measured on a Thomas Hoover melting point apparatus. Reversed-phase HPLC was performed on a Waters system including a 2545 quaternary gradient module pump with a 2489 UV-vis detector and a fraction collector III. An analytical column (4.6 \times 250 mm XBridgeTM BED300 C18, 5 μ m) was used for the purification of all conjugates. For conjugates 3, 4, and 7, a stepwise gradient from 0 to 100% buffer B (0.1% TFA, acetonitrile) in the first 10 min to 50% B and 50% C during the next 10 min to 100% B for the next 10 min was used. Conjugate 5 was purified using a stepwise gradient 0–100% buffer C (0.1% TFA, acetone) with buffer A (0.1% TFA, H₂O) over 45 min. Conjugate 6 was purified using a stepwise gradient 10–90% buffer B with buffer A. Conjugate 8 was purified using a stepwise gradient 70% buffer A and 30% buffer B for 1 min, 20% buffer A and 80% buffer B for 10 min, 10% buffer A and 80% buffer B, 10% buffer C for 12 min, 65% buffer B and 35% buffer C for 25 min, and 70% buffer A and 30% buffer B for 61 min. 5,10,15-Tri(*p*-carboranyl methylthiotetrafluorophenyl)-20-pentafluorophenylpor-

phyrin (**2**) was prepared from TPPF in 30% yield, and conjugate **6** was prepared from porphyrin **2** in 95% yield, as we have recently described.¹⁷ All compounds were obtained in \geq 95% purity, as determined by HPLC (see Supporting Information).

YRFA Synthesis. An Applied Biosystems Pioneer peptide synthesis system was used to synthesize the YRFA peptide using Fmoc-PAL-PEG-PS on a 0.2 mmol scale using the Fmoc strategy of solid-phase peptide synthesis. The first Fmoc-protected amino acid was conjugated to the resin twice in 4-fold excess before loading of the next amino acid in the sequence so as to have 100% loading of the first amino acid and optimize the reaction yield. Coupling reagents HOBr/TBTU were used, and the peptide sequence was monitored using MALDI after cleaving from the resin using a cleavage cocktail TFA/phenol/TIS/H₂O (88:5:2:5).

5,10,15,20-Tetra(*p*-carboranyl methylthiotetrafluorophenyl)-porphyrin (1). To a solution of TPPF (19.5 mg, 0.0200 mmol) in 2 mL of anhydrous DMF were added anhydrous K₂CO₃ (31.5 mg, 0.120 mmol) and mercaptomethyl-*p*-carborane³⁷ (22.8 mg, 0.0800 mmol). The reaction mixture was stirred at room temperature for 48 h. The resulting solution was diluted with ethyl acetate (50 mL) and washed with brine (2 \times 50 mL). The organic layer was dried over anhydrous sodium sulfate, and the solvents were evaporated under reduced pressure. The resulting residue was purified by column chromatography using 3:7 petroleum ether/chloroform for elution, giving 30.0 mg (89%) of the title porphyrin, mp >300 °C. UV-vis (DMSO) λ_{max} ($\epsilon/\text{M}^{-1} \text{cm}^{-1}$) 416 (467 600), 511 (46 800), 555 (19 500), 585 (12 100), 650 (9 200). ¹H NMR (CDCl₃, 400 MHz): δ 8.93 (s, 8H, β -H), 3.47 (s, 8H, SCH₂), 2.16–3.02 (m, 44H, carborane-BH and CH), –2.87 (s, 2H, NH). ¹³C NMR (CDCl₃, 100 MHz): δ 147.78, 147.63, 147.48, 145.30, 145.15, 144.99, 131.93, 131.28, 120.99, 120.80, 120.61, 115.69, 115.50, 115.31, 104.33, 81.87, 59.22, 53.57, 51.82, 40.60, 31.64, 30.93, 29.72, 29.04, 19.15, 14.13. ¹⁹F NMR (acetone-d₆, 233.33 MHz): δ –136.3 to –135.7 (m, 8F), –140.6 to –139.8 (m, 8F). MS (MALDI-TOF) *m/z* calcd for C₅₆H₆₂F₁₆N₄B₄S₄ [M + H]⁺, 1656.773; found, 1656.791.

X-ray Crystallographic Data for Porphyrin 1. Data was collected at 90 K with Cu K α radiation ($\lambda = 1.54178 \text{ \AA}$) on a Bruker Kappa Apex-II diffractometer. C₅₆H₆₂B₄₀F₁₆N₄S₄·2.28CHCl₃, triclinic space group P–1, $a = 12.1535(15)$, $b = 14.690(2)$, $c = 15.015(2) \text{ \AA}$, $\alpha = 71.943(6)$, $\beta = 76.081(9)$, $\gamma = 68.140(8)^\circ$, $V = 2341.5(5) \text{ \AA}^3$, $Z = 1$. One of the two independent carborane cages was disordered into two orientations, with refined occupancies 0.748(5)/0.252(5). The partially occupied carboranes were treated as rigid bodies in the refinement using the geometry of the ordered carborane. The chloroform solvent was disordered, and its contribution to the structure factors was removed using the SQUEEZE procedure. Final R = 0.077, $R_w = 0.229$ for 517 refined parameters and 8266 independent reflections having $\theta_{\text{max}} = 69.6^\circ$. The CIF has been deposited at the Cambridge Crystallographic Data Centre (CCDC 927692).

Porphyrin Conjugate 3. To a solution of porphyrin **2**¹⁷ (14.9 mg, 0.0100 mmol) in 2 mL of NMP was added 4-(2-aminoethyl)-1,7-bis(*tert*-butoxycarbonyl)-1,4,7-triazaheptane (4.50 mg, 0.015 mmol), and the mixture was heated for 4 h at 100 °C. After cooling to room temperature, the solution was diluted with ethyl acetate (50 mL) and washed with brine (5 \times 50 mL). The organic layer was dried over anhydrous sodium sulfate, and the solvents were evaporated under reduced pressure to give a reddish brown residue. This residue was purified by silica gel column chromatography using 9:1 dichloromethane/ethyl acetate for elution to yield pure product (17.0 mg, 96% yield), mp >300 °C. UV-vis (DMSO) λ_{max} ($\epsilon/\text{M}^{-1} \text{cm}^{-1}$) 416 (469 200), 511 (45 200), 555 (18 400), 585 (11 400), 650 (8 100). ¹H NMR (CDCl₃, 400 MHz): δ 9.04 (s, 2H, β -H), 8.92 (s, 6H, β -H), 3.74 (s, 2H, NCH₂), 3.47 (s, 6H, SCH₂), 3.32 (br s, 6H, NCH₂), 2.90 (s, 2H, NCH₂), 2.79 (s, 2H, NCH₂), 1.62–2.68 (m, 33H, carborane-BH and CH), 1.49 (s, 18H, O'Bu), –2.85 (s, 2H, NH). ¹³C NMR (CDCl₃, 100 MHz): δ 156.72, 147.86, 145.16, 138.51, 135.81, 121.04, 115.14, 106.28, 104.07, 81.92, 79.71, 60.77, 59.29, 54.37, 43.05, 40.59, 38.62, 28.78, 21.15, 14.13. ¹⁹F-NMR (acetone-d₆, 233.33 MHz): δ –136.3 to –139.9 to –139.1 (m, 6F), –141.4 (d, $J = 15.9 \text{ Hz}$, 2F), –164.9 (d, $J = 16.3 \text{ Hz}$, 2F). MS (MALDI-TOF) *m/z* calcd for

$C_{69}H_{82}F_{16}N_8B_{30}O_4S_3$ [M]⁺, 1811.839; found, 1811.878. This Boc-protected conjugate was dissolved in 1:1 TFA/dichloromethane (2 mL) in a 10 mL round-bottomed flask and stirred at room temperature for 6 h. The solvent was evaporated under reduced pressure to give a residue, which was purified by HPLC to give 15 mg (95%) of conjugate **3**, mp >300 °C. HPLC t_R = 26.332. UV-vis (DMSO) λ_{max} ($\epsilon/M^{-1} cm^{-1}$) 416 (467 900), 511 (45 300), 555 (18 900), 585 (11 500), 650 (8 100). ¹H NMR (acetone-*d*₆, 400 MHz): δ 9.26 (s, 8H, β -H), 3.58 (s, 6H, SCH₂), 2.23–3.53 (m, 45H, NCH₂, carborane-BH and CH). ¹³C NMR (acetone-*d*₆, 100 MHz): δ 147.76, 145.86, 139.01, 136.11, 122.34, 114.18, 107.18, 102.07, 82.82, 79.91, 61.07, 58.89, 55.07, 43.45, 40.39, 39.12, 29.98, 14.13. ¹⁹F NMR (acetone-*d*₆, 233.33 MHz): δ –136.4 to –135.6 (m, 6F), –139.7 to –138.7 (m, 6F), –140.5 (d, J = 14.7 Hz, 2F), –164.5 (d, J = 13.4 Hz, 2F).

Porphyrin Conjugate 4. To porphyrin **2** (14.9 mg, 0.0100 mmol) in a 10 mL round-bottomed flask were added *N*-(2-aminoethyl)-*N*-[2-[(1,1-dimethylethoxy)carbonyl]amino]ethyl]-1,1-dimethylethyl ester (5.2 mg, 0.015 mmol) and 2 mL of NMP, and the final mixture was heated for 4 h at 100 °C. After cooling to room temperature, ethyl acetate (25 mL) was added to the reaction mixture, and the organic layer was washed five times with brine solution (5 × 25 mL). The resulting mixture was dried over sodium sulfate, and the solvent was evaporated under reduced pressure to give a reddish brown residue. This residue was first passed through silica gel using dichloromethane for elution followed by column chromatography using dichloromethane/ethyl acetate (9:1) to yield pure product (17.5 mg) in 96% yield, mp >300 °C. UV-vis (DMSO) λ_{max} ($\epsilon/M^{-1} cm^{-1}$) 416 (465 800), 511 (44 800), 555 (19 600), 585 (12 900), 650 (8 200). ¹H NMR (CDCl₃, 400 MHz): δ 9.09 (s, 2H, β -H), 8.95 (s, 6H, β -H), 3.90 (s, 2H, NCH₂), 3.85 (s, 2H, NCH₂), 3.42–3.53 (m, 10H, SCH₂, NCH₂), 1.81–2.96 (m, 33H, carborane-BH and CH), –2.83 (s, 2H, NH). ¹³C NMR (CDCl₃, 100 MHz): δ 157.0, 156.28, 147.81, 147.68, 145.33, 145.19, 145.05, 121.69, 121.28, 121.09, 120.90, 120.51, 115.53, 115.34, 115.15, 106.41, 103.99, 103.80, 84.46, 81.91, 81.04, 79.67, 60.42, 59.23, 40.63, 28.43. ¹⁹F NMR (acetone-*d*₆, 233.33 MHz): δ –136.3 to –135.4 (m, 6F), –140.2 to –139.3 (m, 6F), –140.9 (d, J = 16.0 Hz, 2F), –164.8 (d, J = 14.8 Hz, 2F). MS (MALDI-TOF) *m/z* calcd for C₆₇H₇₇F₁₆N₇B₃₀S₃O₄ [M]⁺, 1768.796; found, 1768.783. This Boc-protected conjugate was dissolved in 1:1 TFA/dichloromethane (2 mL) in a 10 mL round-bottomed flask and stirred at room temperature for 6 h. The solvent was evaporated under reduced pressure to give a residue, which was purified by HPLC to give 95.6% (15.5 mg) of conjugate **4**, mp >300 °C. HPLC t_R = 23.866. UV-vis (DMSO) λ_{max} ($\epsilon/M^{-1} cm^{-1}$) 415 (468 000), 511 (45 300), 555 (18 200), 585 (11 800), 650 (8 100). ¹H NMR (acetone-*d*₆, 400 MHz): δ 9.14–9.25 (br s, 8H, β -H), 3.59 (s, 6H, SCH₂), 2.27–3.34 (m, 41H, carborane-BH and CH, NCH₂). ¹³C NMR (acetone-*d*₆, 100 MHz): δ 147.51, 145.23, 145.15, 121.48, 121.29, 120.60, 120.01, 115.14, 115.05, 104.21, 103.90, 84.26, 81.41, 81.02, 79.81, 59.13, 40.63, 14.43. ¹⁹F NMR (acetone-*d*₆, 233.33 MHz): δ –136.6 to –134.8 (m, 6F), –140.2 to –139.4 (m, 6F), –140.1 (d, J = 16.0 Hz, 2F), –164.7 (d, J = 14.1 Hz, 2F).

Porphyrin Conjugate 5. To a solution of porphyrin **2** (14.9 mg, 0.0100 mmol) in 2 mL DMF were added K₂CO₃ (1.1 mg, 0.020 mmol) and 1-thiol- β -D-glucose tetraacetate (5.5 mg, 0.015 mmol). The mixture was stirred for 48 h at room temperature, washed with water (10 mL), and extracted with ethyl acetate (3 × 25 mL). The organic layer was dried over anhydrous sodium sulfate, and the solvent was evaporated under reduced pressure. The product was purified by silica gel column chromatography first using dichloromethane for elution followed by 7:3 dichloromethane/ethyl acetate to give the protected conjugate (17.4 mg) in 95% yield, mp 289–292 °C. UV-vis (DMSO) λ_{max} ($\epsilon/M^{-1} cm^{-1}$) 417 (420 100), 510 (35 700), 555 (17 500), 585 (11 100), 650 (6 800). ¹H NMR (CDCl₃, 250 MHz): δ 9.09 (s, 2H, β -H), 9.01 (s, 6H, β -H), 5.25–5.44 (m, 4H, CH), 4.39 (s, 2H, CH), 3.98 (s, 1H, CH), 3.49 (s, 6H, SCH₂), 1.24–3.26 (m, 45H, carborane-BH and CH, OAc), –2.79 (s, 2H, NH). ¹³C NMR (CDCl₃, 62.5 MHz): δ 170.58, 170.12, 169.41, 169.33, 148.33, 144.36, 131.31, 128.75, 122.03, 121.02, 120.71, 120.41, 115.74, 115.44, 115.13, 112.11, 111.78, 104.29,

103.52, 84.43, 81.77, 73.87, 70.53, 68.01, 61.75, 59.13, 40.47, 20.56. ¹⁹F NMR (CDCl₃, 233.33 MHz): δ –136.2 to –135.4 (m, 6F), –139.8 to –138.0 (m, 6F), –144.2 (d, J = 18.6 Hz, 2F), –162.8 (d, J = 17.2 Hz, 2F). To a solution of the above compound (17.4 mg, 0.0095 mmol) in 10 mL of 1:1 chloroform/methanol was added 50 μ L of 0.5 M NaOMe in methanol, and the final solution was stirred at room temperature for 2 h. The solvents were evaporated under reduced pressure to give a red color residue, which was purified by silica gel chromatography first using dichloromethane for elution followed by 3:7 dichloromethane/ethyl acetate. The pure conjugate was obtained (14.68 mg) in 93% yield, mp 289–292 °C. HPLC t_R = 19.433. UV-vis (DMSO) λ_{max} ($\epsilon/M^{-1} cm^{-1}$) 417 (440 010), 510 (37 600), 555 (17 500), 585 (11 100), 650 (9 100). ¹H NMR (CDCl₃, 250 MHz): δ 8.94 (s, 2H, β -H), 8.86 (s, 6H, β -H), 5.32 (br s, 4H, OH), 4.81 (br s, 1H), 4.07–4.21 (m, 4H, CH), 3.81 (s, 1H, CH), 1.43–3.60 (m, 39H, carborane-BH and CH, SCH₂). ¹³C NMR (CDCl₃, 62.5 MHz): δ 148.26, 144.26, 130.84, 120.50, 120.41, 115.25, 112.29, 104.19, 86.83, 81.58, 79.97, 73.74, 69.43, 61.91, 58.90, 40.46, 40.14, 29.58. ¹⁹F NMR (acetone-*d*₆, 233.33 MHz): δ –135.7 to –134.9 (m, 6F), –140.0 to –139.3 (m, 6F), –144.9 (d, J = 19.6 Hz, 2F), –162.4 (d, J = 14.2 Hz, 2F).

Porphyrin Conjugate 7. To a solution of conjugate **6**¹⁷ (16.9 mg, 0.0100 mmol) in 0.5 mL DMF was added DIEA (7.8 mg, 0.060 mmol), and the mixture was stirred for 10 min at room temperature. HATU (3.82 mg, 0.0100 mmol) was added, and stirring was continued for 15 min. L-Arginine amide dihydrochloride (2.4 mg, 0.010 mmol) was added, and the final reaction mixture was stirred for 48 h at 37 °C. The solvent was removed under reduced pressure, and the resulting residue was purified by HPLC to give 15.6 mg (85% yield) of conjugate **7**, mp >300 °C. HPLC t_R = 25.856. UV-vis (DMSO) λ_{max} ($\epsilon/M^{-1} cm^{-1}$) 416 (458 100), 511 (44 100), 555 (17 100), 585 (11 100), 650 (7 500). ¹H NMR (acetone-*d*₆, 400 MHz): δ 8.9–9.5 (br s, 8H, β -H), 3.29–3.91 (m, 25H, SCH₂, NCH₂, arginine-CH₂ and CH, OCH₂), 1.78–3.07 (m, 45H, arginine-CH₂, carborane-BH and CH). ¹³C NMR (acetone-*d*₆, 100 MHz): δ 173.20, 171.48, 157.95, 148.60, 145.65, 121.04, 115.14, 106.53, 104.31, 70.32, 70.24, 70.15, 70.06, 67.0, 59.89, 51.31, 40.47, 36.23, 24.80, 22.42, 13.46. ¹⁹F NMR (acetone-*d*₆, 233.33 MHz): δ –135.2 to –134.6 (m, 6F), –139.6 to –138.9 (m, 6F), –140.8 (d, J = 15.4 Hz, 2F), –164.1 (d, J = 12.1 Hz, 2F).

Porphyrin Conjugate 8. A solution of conjugate **6**¹⁷ (16.91 mg, 0.01 mmol) in DMF (0.5 mL) and DIEA (7.8 mg, 0.06 mmol) was stirred for 10 min at room temperature. HOBT (1.5 mg, 0.01 mmol) and DEPBT (3.0 mg, 0.01 mmol) were added, and the mixture was stirred at room temperature for another 15 min. The activated porphyrin was added to the peptide on PAL-PEG-PS resin (5.6 mg, 0.01 mmol), and the final mixture was stirred for 96 h. Then, the resin was washed under vacuum several times with DMF followed by methanol and DCM. A cleavage cocktail, TFA/phenol/TIS/H₂O (88:5:2:5), was added with constant shaking for 4 h. Then, the mixture was washed with TFA into a flask and concentrated under vacuum. Cold diethyl ether was added to the residue, and the mixture was centrifuged. The obtained red colored solid was purified by HPLC to yield 7 mg (65%) of conjugate **8**, mp > 300 °C. HPLC t_R = 25.698. UV-vis (DMSO) λ_{max} ($\epsilon/M^{-1} cm^{-1}$) 416 (462 100), 511 (44 300), 555 (17 900), 585 (12 100), 650 (8 100). ¹H NMR (acetone-*d*₆, 400 MHz): δ 9.4 (s, 2H, β -H), 9.32 (s, 6H, β -H), 7.16–7.28 (m, 4H, o-Ph-H), 7.13 (s, 1H, p-Ph-H), 7.03–7.10 (d, J = 3.44 Hz, 2H, m-Ph-H), 6.72–6.79 (d, J = 4.56 Hz, 2H, m-Ph-H), 3.85–4.01 (m, 4H, OCH₂), 3.63–3.78 (m, 12H, OCH₂), 3.6 (s, 6H, SCH₂), 3.4–3.51 (m, 6H, NCH₂), 1.3–3.21 (m, 56H, carborane-BH and CH, peptide-CH), –2.89 (s, 2H, NH). ¹³C NMR (acetone-*d*₆, 100 MHz): δ 172.47, 162.62, 159.01, 158.62, 156.72, 148.11, 145.65, 138.27, 130.33, 129.25, 128.19, 126.32, 123.95, 117.22, 115.24, 114.36, 81.68, 70.12, 66.92, 60.03, 56.58, 55.60, 52.65, 45.27, 40.34, 36.65, 35.67, 26.57, 24.60, 19.43. ¹⁹F NMR (acetone-*d*₆, 233.33 MHz): δ –135.6 to –134.8 (m, 6F), –140.1 to –139.0 (m, 6F), –140.9 (d, J = 15.9 Hz, 2F), –164.7 (d, J = 16.5 Hz, 2F). MS (MALDI-TOF) *m/z* calcd for C₈₀H₁₀₃F₁₆N₁₃B₃₀S₃O₉ [M + H]⁺, 2224.990; found, 2224.998. MS-MS (MALDI-TOF-TOF) *m/z* calcd for C₈₉H₉₈F₁₆N₁₂B₃₀S₃O₉,

2205.807; $C_{85}H_{96}F_{16}N_{11}B_{30}S_3O_7$, 2108.591; $C_{71}H_{77}F_{16}N_7B_{30}S_3O_6$, 1888.408; $C_{70}H_{76}F_{16}N_8B_{30}S_3O_5$, 1805.461; found, 2224.998 [Por-PEG-YRFA-CONH₂ + H]⁺, 2205.800 [(PorPEG-YRFA-CO) - 2H]⁺, 2108.591 [PorPEG-YRF], 1888.405 [(PorPEG-Y-CONH₂ + K + H]⁺, 1805.420 [PorPEG-Y].

Cell Studies. All tissue culture medium and reagents were purchased from Invitrogen (Carlsbad, CA). Human glioma T98G cells were purchased from ATCC and cultured in ATCC-formulated Eagle's minimum essential medium containing 10% FBS and 1% antibiotic (penicillin/streptomycin). The hCMEC/D3 cells were obtained from coauthors from the Institut COCHIN (Paris, France). All compound solutions were filter-sterilized using a 0.22 μ m syringe filter.

Dark Cytotoxicity. Human T98G cells (10 000 per well) were plated in a Costar 96-well plate and allowed to grow for 36 h. Conjugate stock solutions (32 mM) were prepared in DMSO and then diluted into final working concentrations (25, 50, 100, 200, 400 μ M). The cells were exposed to increasing concentrations of porphyrin conjugate up to 400 μ M and incubated overnight. The loading medium was removed, and the cells were washed with 100 μ L of PBS. Medium containing CellTiter Blue (Promega) (120 μ L) was added as per the manufacturer's instructions. After a 4 h incubation, the cytotoxicity was measured by reading the fluorescence at 520/584 nm using a BMG FLUOstar plate reader. The signal was normalized to 100% viable (untreated) cells and 0% viable (treated with 0.2% saponin from Sigma) cells.

Phototoxicity. Human T98G cells were prepared as described above and treated with conjugate concentrations of 0, 6.25, 12.5, 25, 50, and 100 μ M. After compound loading, the medium was removed and replaced with medium containing 50 mM HEPES, pH 7.4. The cells were exposed to a NewPort light system containing a 175 W halogen lamp for 20 min, filtered through a water filter to provide an approximately 1.5 J/cm² light dose. The cells were kept cool by placing the culture on a 50C Echotherm chilling/heating plate (Torrey Pines Sci. Inc.). The cells were returned to the incubator overnight and assayed for cytotoxicity as described above.

Time-Dependent Uptake. Human T98G cells were prepared as described above and exposed to 10 μ M of each conjugate for 0, 1, 2, 4, 8, and 24 h. At the end of the incubation period, the loading medium was removed, and the cells were washed with 200 μ L of PBS. The cells were solubilized upon addition of 100 μ L of 0.25% Triton X-100 (Calbiochem) in PBS. To determine the porphyrin concentration, fluorescence emission was read at 415/650 nm (excitation/emission) using a BMG FLUOstar plate reader. The cell number was quantified using the CyQuant cell proliferation assay (Invitrogen) as per the manufacturer's instructions, and the uptake was expressed in terms of compound concentration (nanomolar) per cell.

Microscopy. Human HEp2 cells were incubated in a glass bottom 6-well plate (MatTek) and allowed to grow for 48 h. The cells were exposed to 10 μ M of each porphyrin conjugate for 6 h. Organelle tracers were obtained from Invitrogen and used at the following concentrations: LysoSensor Green, 50 nM; MitoTracker Green, 250 nM; ER Tracker Blue/White, 100 nM; and BODIPY FL C5 Ceramide, 1 mM. The organelle tracers were diluted in medium, and the cells were incubated concurrently with conjugate and tracers for 30 min before washing three times with PBS and imaging by microscopy. Images were acquired using a Leica DM RXA2 upright microscope with 40X NA 0.8 dip objective lens and DAPI, GFP, and Texas Red filter cubes (Chroma Technologies).

hCMEC/D3 Cell Line (In Vitro BBB Model). The human brain capillary endothelial hCMEC/D3 cells were incubated in a 6-well, 0.4 μ m porosity PET transwell plate (Corning) and allowed to grow for 48 h to form a model BBB monolayer. EBM-2 medium containing 5% FBS, 1% penicillin/streptomycin, hydrocortisone, ascorbic acid, chemically defined lipid concentrate (1/100), HEPES, and bFGF was used as growth medium. A 0.5 mL sample of each porphyrin conjugate or standard lucifer yellow (LY) at 1 mg/mL concentration in HBSS (pH 6.7–7.8) was added to the upper chamber (mimicking the blood compartment), and 1.5 mL of HBSS buffer was added to the lower chamber (mimicking the cerebral compartment), see Supporting

Information, Figure S10. The cells were incubated (37 °C, 95% humidity, 5% CO₂) for 0, 30, and 60 min, and at the end of each incubation time, 5 \times 100 μ L of solution from the lower chamber was pipetted out, and 500 μ L of fresh HBSS buffer was added back to the lower chamber. The five 100 μ L (five replicates) solutions that were collected from the lower chamber were added to a 96-well plate. The porphyrin and LY concentrations were determined by fluorescence emission, read at 415/650 nm and 420/540 nm (excitation/emission), respectively, using a BMG FLUOstar plate reader. The permeability coefficients (P) were determined following the clearance principle, according to the equation below,³⁸ where C_f is the final concentration of the compound (ng/mL), C_0 is the initial concentration of compound (ng/mL), t_f is the final time (min), t_0 is the initial time (min), and A is the surface area of the filter (cm²).

$$P = \frac{(C_f - C_0)}{(t_f - t_0)} \times \frac{1}{A \cdot C_0 \cdot 60}$$

RESULTS AND DISCUSSION

Synthesis and Characterization. Commercially available TPPF was the starting material used for the preparation of the *p*-carborane-containing porphyrins 1–8, as shown in Scheme 1. The nucleophilic substitution of the *p*-fluorine groups of TPPF is a convenient strategy for the synthesis of functionalized porphyrins for therapeutic and other applications.²¹ Reaction of TPPF with 6 equiv of 1-mercaptopethyl-*p*-carborane³⁷ in DMF and in the presence of K₂CO₃ produced the symmetric tetra(carboranyl)porphyrin 1 in 89% yield. The tri(carboranyl)-porphyrin 2 was obtained using 4 equiv of 1-mercaptopethyl-*p*-carborane, as we recently reported,¹⁷ and was used for the preparation of conjugates 3–8. The *p*-carborane clusters were chosen as the source of boron in these porphyrins due to their higher stability toward deboronation in the presence of bases and nucleophiles compared to that of the most commonly used *o*-carboranes.^{16,39} Slow recrystallization of porphyrin 1 by slow diffusion of hexane into chloroform gave crystals suitable for X-ray analysis. As shown in Figure 2, the molecule lies on an inversion center in the crystal, and the porphyrin core is nearly planar, with the best plane of its 24 atoms having a mean

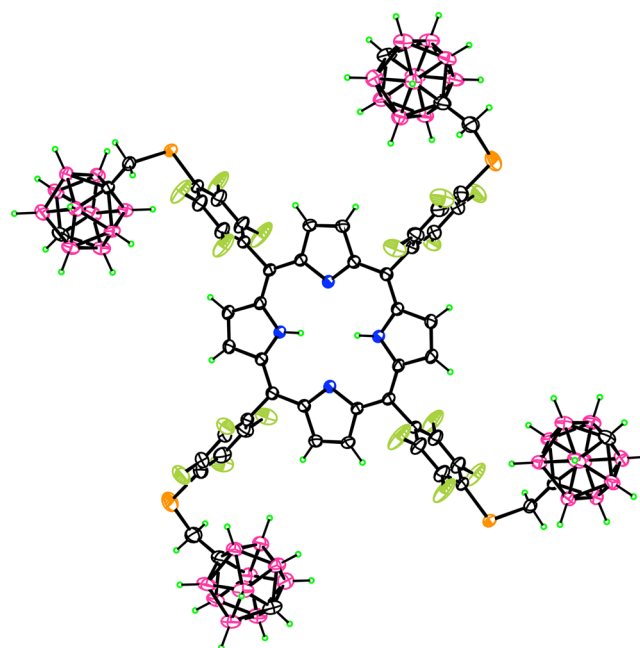


Figure 2. X-ray crystal structure of porphyrin 1.

deviation of 0.022 Å and a maximum of 0.048(4) Å. The phenyl planes are nearly orthogonal to the porphyrin plane, forming dihedral angles of 89.1(1) and 83.8(1)° with it. The four sulfur atoms are coplanar and approximate a square (13.46 Å per side). The centroids of the *p*-carborane cages are nearly in the porphyrin plane, lying alternately 0.60 Å above and 0.90 Å below it. One of the two independent *p*-carborane cages is disordered into two orientations in approximately 3:1 ratio (not shown in Figure 1). This is the first and only structure of a porphyrin-bearing *p*-carborane in the Cambridge Structural Database (CSD),⁴⁰ although 16 structures have appeared of porphyrins with *o*-carborane. These tend to have structures similar to that of 1, with near-planar porphyrin cores, frequently lying on inversion centers. However, in a few of these *o*-carboranylporphyrins, steric effects⁴¹ or substitution patterns of lower symmetry⁴² lead to nonplanar porphyrin cores.

Substitution of the *p*-fluorophenyl group of porphyrin 2 with the primary amine group of commercially available Boc-protected polyamines (linear and branched polyamines), 1-thiol- β -D-glucose tetraacetate, and *tert*-butyl-12-amino-4,7,10-trioxadodecanoate, followed by deprotection, gave the corresponding conjugates 3–6 in nearly quantitative yields (>95%) after reverse-phase HPLC purification. The carboxyl-terminated tri(ethylene glycol)porphyrin 6¹⁷ was conjugated in solution phase to L-arginine, using HATU and DIEA, to produce conjugate 7 in 89% yield and in solid phase to YRFA, using DEPBT, HOBr, and DIEA, to produce 8 in 65% yield after HPLC purifications.

One linear and one branched (containing an additional aminoethyl moiety) polyamine was conjugated to porphyrin 2 to evaluate the effect of their chemical structure and overall cationic charge on cytotoxicity, cellular uptake, and BBB permeability. The arginine conjugate 7 was prepared for comparison purposes because the guanidinium group has been previously observed to enhance binding to phosphate-containing plasma membranes and to increase cellular uptake.^{26,27} The tri(ethylene glycol) group in conjugates 7 and 8 increases the solubility of porphyrin macrocycles and has been shown to further enhance their cellular uptake.^{27,43} The glucose conjugate 5 was prepared to investigate the potential targeting of lectins and of glucose transporters (GLUT) overexpressed on tumor cells and the BBB.^{30–32} YRFA is a tetrapeptide with the sequence Tyr-D-Arg-Phe- β -Ala with demonstrated high affinity and selectivity for μ -opioid receptors as well as good enzymatic stability.^{34–36}

Studies in T98G cells. Cytotoxicity. The concentration-dependent dark and phototoxicity of all porphyrin conjugates were investigated in T98G cells, and the results are summarized in Table 1 (see also Figures S8 and S9 of the Supporting Information). None of the conjugates were toxic to cells, with determined IC₅₀ > 400 μ M in the dark and IC₅₀ > 100 μ M upon irradiation with a low light dose (1.5 J/cm²). These results are in agreement with our previous studies on a series of spermine derivatives 9–15¹⁷ (see Figure 1) and of cobaltabisdicarbollide-containing porphyrins conjugated to a PEG⁴³ or arginine-rich peptide¹⁸ that showed low toxicities, probably as a result of the attachment of the carborane clusters to the macrocycle rather than to the biomolecule. The observed low cytotoxicity of this series of compounds is important for their use as boron-delivery agents because of the high boron concentration requirement in BNCT (>20 μ g/g weight), and their low phototoxicity makes them unsuitable for application as PDT photosensitizers.

Table 1. Cytotoxicity^a for Porphyrin Conjugates Using Human Glioma T98G Cells and Major Localization Sites in Human HEp2 Cells

| compd | dark toxicity IC ₅₀ (μ M) | phototoxicity IC ₅₀ (μ M) | major sites of localization |
|-----------------|---|---|-----------------------------|
| 1 | >400 | >100 | Lyso, Mito, Golgi |
| 3 | >400 | >100 | Mito, Golgi, ER |
| 4 | >400 | >100 | Lyso, Mito, Golgi |
| 5 | >400 | >100 | Lyso, Mito, Golgi |
| 6 ¹⁷ | 296 | >100 | Lyso, Mito, ER |
| 7 | >400 | >100 | Lyso, Mito, Golgi |
| 8 | >400 | >100 | Lyso, Mito, Golgi |

^aCellTiter Blue assay; light dose ~ 1.5 J/cm².

Cellular Uptake. The time-dependent uptake of conjugates 1, 3, 4, 5, 7, and 8 into glioma T98G cells was evaluated at a concentration of 10 μ M over 24 h, and the results are shown in Figure 3. All conjugates accumulated rapidly within cells in the

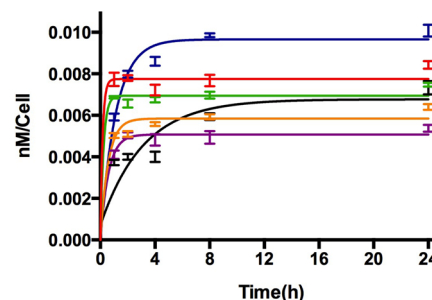


Figure 3. Time-dependent uptake of porphyrin 1 (red) and conjugates 3 (green), 4 (orange), 5 (black), and 8 (purple) at 10 μ M by human glioma T98G cells.

first 2 h, after which a plateau was reached except for the glucose conjugate 5, which showed continuous uptake over the 24 h period investigated, suggesting GLUT-mediated transport. At 4, 8, and 24 h, the L-arginine conjugate 7 showed the highest uptake followed by the tetracarboranylporphyrin 1. We have previously observed that the cellular uptake depends on the number of carborane clusters at the periphery of the porphyrin macrocycle^{44,45} and that tetracarboranylporphyrins tend to accumulate to a higher extent than their tricarboranylporphyrin analogues^{18,44} as a result of their increased hydrophobicity. We have also reported that the extent of cellular uptake of polyamine conjugates 9–15¹⁷ (Figure 1) generally increases with the hydrophilicity of the conjugates and that compared with that of 9, conjugates 10 and 11, bearing additional aminoethyl moieties, are taken up more efficiently by T98G cells. In agreement with these observations, the branched polyamine conjugate 3 showed higher uptake at all time points investigated compared with that of conjugate 4, probably as a result of its greater positive charge and hydrophilicity. On the other hand, the most efficiently internalized at times >4 h was the L-arginine conjugate 7, probably due to the unique ability of the guanidinium group to form bidentate hydrogen bonds with membrane-containing phosphates, as we and many others have previously observed.^{26,27,46}

Intracellular Localization. To investigate the main sites of intracellular localization of the conjugates, fluorescence microscopy was conducted using HEp2 rather than T98G cells because the former spread nicely on glass coverslips, facilitating imaging. The organelle-specific fluorescent probes

ERTracker Blue/White (ER), MitoTracker Green (mitochondria), BODIPY-FL Ceramide (Golgi), and Lysosensor Green (lysosomes) were used in the overlay experiments, as shown in Figures 4 and 5 (for conjugates 3 and 8, respectively) and in the Supporting Information, Figures S12–S15 (for porphyrins 1, 4, 5, and 7, respectively); the data are also summarized in Table 1. The polyamine conjugates localized preferentially in mitochondria, Golgi, and ER, the glucose conjugate **5** was mainly found in the lysosomes and mitochondria, and the arginine and YRFA conjugates were mainly found in the lysosomes, Golgi, and mitochondria. These results are in agreement with our previous observations on the intracellular distribution of porphyrin conjugates.^{17,18,26,27} The multiple sites of intracellular localization observed for these porphyrins could lead to damage to multiple intracellular sites, resulting in more effective tumor cell destruction.

BBB Permeability Studies in hCMEC/D3 cells. The hCMEC/D3 cell line retains most of the morphological and functional characteristics of human brain endothelial cells, including many of the drug transporters found in human BBB, and it is believed to be an excellent model for studies of BBB function and drug transport processes.^{47–51} The transport of boron-containing molecules across the BBB is largely hindered, which poses a major challenge in BNCT upon systemic drug delivery, and the observed selective uptake of certain boronated porphyrins into brain tumor is believed to be due to the breakdown of the BBB within the tumor region, whereas an intact BBB prevents the uptake in normal brain.⁵² Because free diffusion across the BBB is limited to a small number of compounds of low molecular weight (<400 Da), we hypothesized that conjugation of a carboranylporphyrin to molecules that target BBB receptors (GLUT and μ -opioid) or macrocycles containing cationic groups for enhanced interactions with membrane phosphates could increase their transport across brain endothelial cells. The transport of several molecules across hCMEC/D3 cell monolayers, including sugars, flavonoids, liposomes, and oligopeptides, have been previously reported, and several receptors and transporters have been identified,^{53–58} including P-glycoprotein (P-gp), breast cancer resistance protein (BCRP), multidrug resistance-associated proteins (MRP), solute carriers (SLC), and proton-coupled oligopeptide transporters (POT). However, this BBB model has not previously been used for the investigation of boron-delivery agents for BNCT or of porphyrin derivatives.

To investigate the BBB permeability of our carboranylporphyrin **1** and conjugates **3–15**, we used the hCMEC/D3 cell line as an *in vitro* model for the human BBB, comparing their permeability to that of standard lucifer yellow (LY), a small fluorescent molecule with a 429 Da molecular weight and 536 nm emission that contains two sulfonates and one cabohydrazine group. The BBB model (see Supporting Information, Figure S10) consists of a basolateral chamber (mimicking the cerebral compartment) and an apical chamber (mimicking the blood compartment) containing a monolayered cell membrane to which the porphyrins were added. The permeability studies were completed within 1 h to ensure that the cell monolayer retained its function and integrity in the absence of cell medium. The permeabilities of the porphyrin conjugates are given as permeability coefficients (*P*), determined as previously described.³⁸ Table 2 summarizes the *P* values obtained for LY and the porphyrin conjugates **1** and **3–15**. The *P* value obtained for LY is in agreement with that reported in the

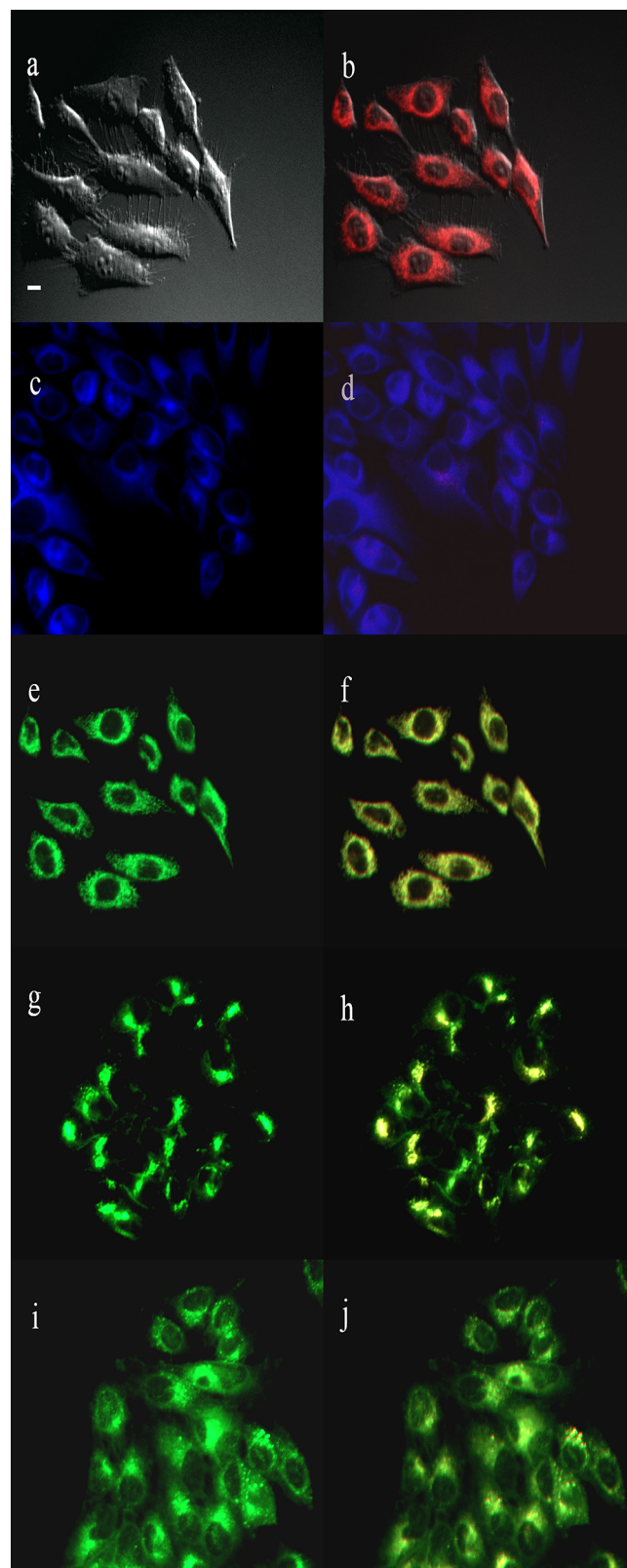


Figure 4. Subcellular fluorescence of conjugate **3** in HEp2 cells at 10 μ M for 6 h: (a) phase contrast, (b) overlay of the fluorescence of **3** and phase contrast, (c) ER Tracker Blue/White fluorescence, (e) MitoTracker Green fluorescence, (g) BODIPY Ceramide, (i) Lysosensor Green fluorescence, and (d, f, h, j) overlays of organelle tracers with the fluorescence of **3**. Scale bar, 10 μ m.

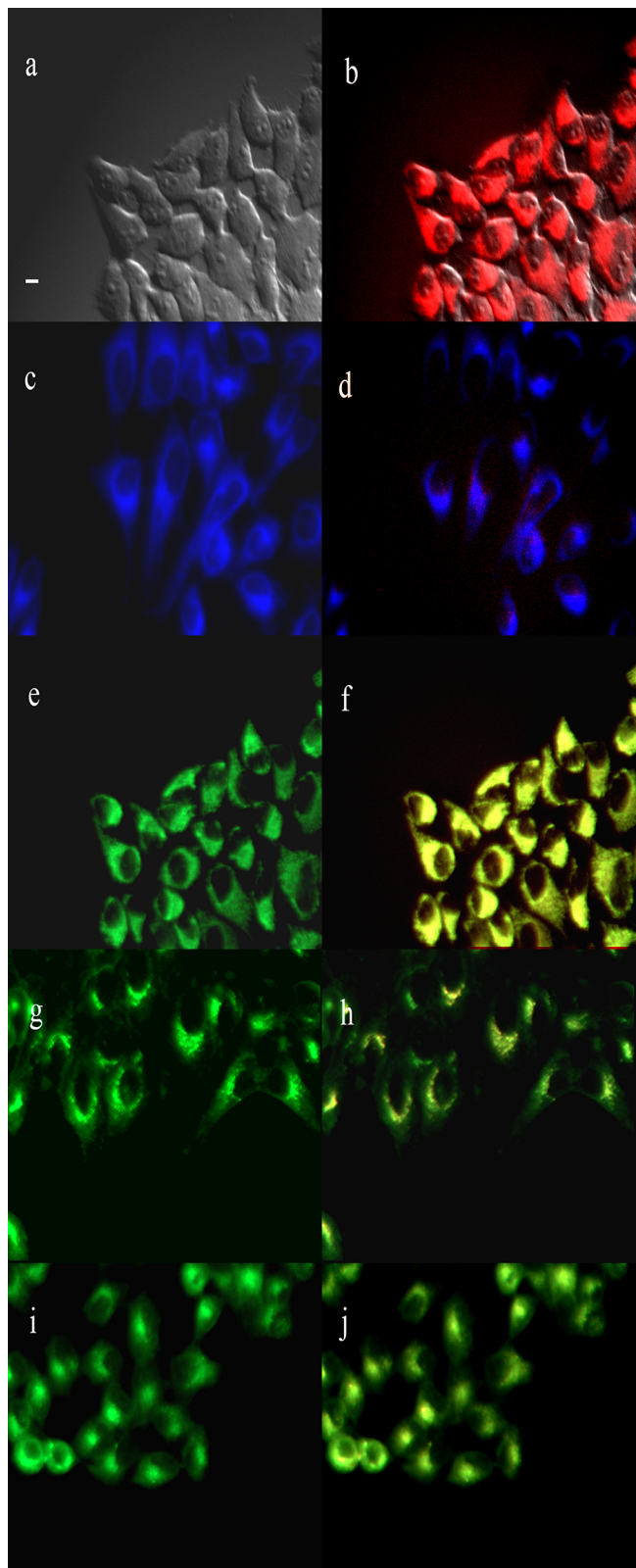


Figure 5. Subcellular fluorescence of conjugate 8 in HEp2 cells at 10 μM for 6 h: (a) phase contrast, (b) overlay of the fluorescence of 8 and phase contrast, (c) ER Tracker Blue/White fluorescence, (e) MitoTracker Green fluorescence, (g) BODIPY Ceramide, (i) Lysosensor Green fluorescence, and (d, f, h, j) overlays of organelle tracers with the fluorescence of 8. Scale bar, 10 μm .

Table 2. Permeability Coefficients (P) for Porphyrin Conjugates and Lucifer Yellow (LY) Using Human Endothelial hCMEC/D3 Cells

| compd | $P \times 10^{-6}$ (cm/s) |
|-------|---------------------------|
| 1 | 1.36 \pm 0.04 |
| 3 | 2.32 \pm 0.02 |
| 4 | 0.82 \pm 0.02 |
| 5 | 0.62 \pm 0.05 |
| 6 | 1.18 \pm 0.03 |
| 7 | 1.44 \pm 0.03 |
| 8 | 1.71 \pm 0.06 |
| 9 | 1.31 \pm 0.08 |
| 10 | 0.82 \pm 0.06 |
| 11 | 1.21 \pm 0.04 |
| 12 | 3.29 \pm 0.03 |
| 13 | 1.10 \pm 0.06 |
| 14 | 0.87 \pm 0.08 |
| 15 | 1.47 \pm 0.05 |
| LY | 21.7 \pm 0.30 |

literature,^{48,49} and the lower P values measured for all porphyrin conjugates reflect the integrity of the brain endothelial monolayer. The permeability of molecules across hCMEC/D3 cell monolayers depends on molecular weight, hydrophobic character, and the targeting of specific receptors on the cell surface. The higher molecular weight for all porphyrin conjugates in comparison with that of LY along with their higher hydrophobic character and tendency for aggregation in aqueous conditions⁴⁵ account for their lower permeability coefficients in comparison with that of LY. Within the series of porphyrins investigated, the polyamine conjugates 3 and 12 showed higher P values, followed by the YRFA conjugate 8, whereas conjugate 5 had the lowest P value. It is interesting that porphyrins 1 and 3 with the highest uptake into T98G cells after 1 h (see Figure 2) also showed high permeability, whereas conjugate 5, the least taken up by T98G cells after 1 h, showed the lowest permeability. In addition, the observed permeability is enhanced for the branched polyamine conjugate 3 in comparison with that of the linear polyamine conjugate 4 containing one less ethylamine arm, as was also observed in the uptake into T98G cells (Figure 2). These results suggest that the glucose conjugate 5 is not targeting the GLUT receptors expressed at the surface of hCMEC/D3 cells, which might be due to its tendency for aggregation in aqueous solutions. On the other hand, it has been previously observed that the hCMEC/D3 cells express amino acid and oligopeptide transporters, such as hPHT1 and hPHT2, whereas they express little or no hPepT1 and hPepT2,⁵⁹ and no studies were conducted on the expression of μ -opioid receptors. The higher P value found for the opioid-targeted YRFA conjugate 8 compared with those of untargeted porphyrins 1 and 6 as well as the P values found for most polyamine conjugates, with the exception of 3 and 12, suggests that conjugate 8 might be targeting receptors on the cell surface. It is possible that positively charged conjugates have enhanced interactions with negatively charged cell membranes, favoring their transport across the cell monolayer. Indeed, the arginine conjugate 7 showed increased permeability compared with its precursor porphyrin-PEG 6. It is also interesting to note that among the polyamine series 12–15 that differ only in the number of carbon spacers between the amine groups, conjugate 12 containing the smallest carbon backbone (2–3–2) showed

the highest permeability, whereas **14**, with the largest backbone (3–4–3), showed the lowest.

The above results show that the hCMEC/D3 cells form a tight BBB-like monolayer that restricts the permeability of boron-containing porphyrins. Previous studies have shown that monolayers of this brain endothelial cell line indeed restrict the uptake of many hydrophobic and hydrophilic molecules,^{47–51} correlating with in vivo studies. An approach to overcome the low permeability of drugs across the BBB is the use of carrier systems that are endocytosed by brain endothelial cells upon receptor binding, such as immunoliposomes and other targeted nanoparticles. Studies using hCMEC/D3 cells and drug-encapsulated targeted nanoparticles have shown increasing drug delivery across the BBB monolayer,^{49,55} and this might be a more efficient methodology for delivering boron to the brain.

CONCLUSIONS

We describe the synthesis and in vitro studies of a series of tri[(*p*-carboranyl methylthio)tetrafluorophenyl]porphyrin conjugates to glucose, arginine, linear and branched polyamines, and tri(ethylene glycol)-YRFA. The *p*-carborane groups, unlike the most common *o*-carboranes, are stable under the basic and coupling conditions used to prepare the conjugates. A tetra[(*p*-carboranyl methylthio)tetrafluorophenyl]porphyrin was also synthesized, and its crystal structure is the first in the CSD of a porphyrin-bearing *p*-carborane clusters.

None of the porphyrin conjugates were toxic to human glioma T98G cells, both in the dark ($IC_{50} > 400 \mu M$) and upon exposure to 1.5 J/cm^2 light ($IC_{50} > 100 \mu M$), an important feature of boron-delivery agents because of the high amount of boron needed in BNCT ($>20 \mu \text{g/g tumor}$). Within this series of porphyrins, the tetra(*p*-carboranyl methylthio)porphyrin **1** and the branched polyamine conjugate **3** accumulated the fastest in T98G cells, but after 2 h, a plateau was reached, whereas the arginine and glucose conjugates continued to accumulate over time. At times >4 h, the arginine conjugate **7** had the highest uptake into cells, whereas the YRFA conjugate **8** had the least. The glucose conjugate **5** was taken up the slowest in this series, but at times >8 h it showed similar uptake as that of the polyamine conjugates. All compounds localized in multiple organelles within human HEp2 cells, including the mitochondria, lysosomes, Golgi, and ER, suggesting the potential for multiple sites of damage upon neutron irradiation.

The hCMEC/D3 cells formed a tight BBB-like monolayer that restricted the permeability of the porphyrin conjugates, as indicated by their lower permeability coefficients than that of LY, as a result of their relatively high molecular weights, hydrophobicity, and tendency for aggregation. This is the first investigation of the BBB permeability of boron-containing porphyrins in an in vitro model. The hCMEC/D3 model is easy and convenient to use, allowing high-throughput testing and comparison of potential BNCT agents at times up to 1 h (to ensure the integrity of the cell monolayer). The permeability coefficients for the porphyrin conjugates followed the order **12** $>$ **3** $>$ **8** \sim **15** $>$ **9** \sim **1** $>$ **11** \sim **6** $>$ **13** $>$ **4** \sim **10** \sim **14** $>$ **5**. The polyamine conjugates **12** and **3** showed the highest permeability coefficients, probably as a result of enhanced interactions with negatively charged cell membranes, followed by the YRFA conjugate **8**, which could be targeting receptors on the cell membrane. On the other hand, the glucose conjugate **5** showed the lowest permeability, due to its poor aqueous solubility and its tendency for aggregation, which prevents the targeting of GLUT receptors expressed at the

surface of hCMEC/D3 cells; this result is also in agreement with its observed lower uptake into T98G cells at early time points. Our studies show that certain cationic polyamine and arginine porphyrin conjugates, as well as the YRFA conjugate, bearing stable *p*-carborane clusters are promising boron-delivery vehicles for BNCT of brain tumors.

ASSOCIATED CONTENT

Supporting Information

HPLC conditions and chromatograms, fluorescence spectra, cytotoxicity, uptake, and microscopy figures as well as NMR and MS data. This material is available free of charge via the Internet at <http://pubs.acs.org>.

AUTHOR INFORMATION

Corresponding Author

*Phone: 225-578-7405. Fax: 225-578-3458. E-mail: vicente@lsu.edu.

Notes

The authors declare no competing financial interest.

ACKNOWLEDGMENTS

This work was partially supported by the National Institutes of Health, award nos. R01 CA098902 and R25GM069743.

ABBREVIATIONS USED

BNCT, boron neutron capture therapy; BBB, blood–brain barrier; PDT, photodynamic therapy; TPPF, 5,10,15,20-tetrakis(2,3,4,5,6-pentafluorophenyl)porphyrin; CSD, Cambridge Structural Database; TFA, trifluoroacetic acid; LET, linear energy transfer; PBS, phosphate buffered saline; EBM-2, endothelial cell basal medium 2; bFGF, human basic fibroblast growth factor; HBSS, Hank's balanced salt solution; FBS, fetal bovine serum; NMP, *N*-methylpyrrolidone; DIEA, *N,N*-diisopropylethylamine; HATU, 2-(7-aza-1*H*-benzotriazole-1-yl)-1,1,3,3-tetramethyluronium hexafluorophosphate; HEPES, 2-[4-(2-hydroxyethyl)piperazin-1-yl]ethanesulfonic acid; DMEM, Dulbecco's modified Eagle's medium; ER, endoplasmic reticulum; DEPBT, 3-(diethoxy-phosphoryloxy)-3*H*-benzo[1,2,3]triazin-4-one; TIS, triisopropyl silane; TBTU, *O*-(benzotriazol-1-yl)-*N,N,N',N'*-tetramethyluronium tetrafluoroborate

REFERENCES

- (1) Soloway, A. H.; Tjarks, W.; Barnum, B. A.; Rong, F. G.; Barth, R. F.; Codogni, I. M.; Wilson, J. G. The chemistry of neutron capture therapy. *Chem. Rev.* **1998**, *98*, 1515–1562.
- (2) Barth, R. F.; Coderre, J. A.; Vicente, M. G. H.; Blue, T. E. Boron neutron capture therapy of cancer: current status and future prospects. *Clin. Cancer Res.* **2005**, *11*, 3987–4002.
- (3) Barth, R. F.; Vicente, M. G. H.; Harling, O. K.; Kiger, W. S., III; Riley, K. J.; Binns, P. J.; Wagner, F. M.; Suzuki, M.; Aihara, T.; Kato, I.; Kawabata, S. Current status of boron neutron capture therapy of high grade gliomas and recurrent head and neck cancer. *Radiat. Oncol.* **2012**, *7*, 146–167.
- (4) Kankaanranta, L.; Seppälä, T.; Koivunoro, H.; Saarilahti, K.; Atula, T.; Collan, J.; Salli, E.; Kortesniemi, M.; Uusi-Simola, J.; Välimäki, P.; Mäkitie, A.; Seppänen, M.; Minn, H.; Revitzer, H.; Kouri, M.; Kotiluoto, P.; Seren, T.; Auterinen, I.; Savolainen, S.; Joensuu, H. Boron neutron capture therapy in the treatment of locally recurred head-and-neck cancer: final analysis of a phase I/II trial. *Int. J. Radiat. Oncol., Biol., Phys.* **2012**, *82*, e67–e75.
- (5) Barth, R. H.; Vicente, M. G.; Harling, O.; Kiger, W.; Riley, K.; Binns, P.; Wagner, F.; Suzuki, M.; Aihara, T.; Kato, I.; Kawabata, S.

- Current status of boron neutron capture therapy of high grade gliomas and recurrent head and neck cancer. *Radiat. Oncol.* **2012**, *7*, 146.
- (6) Hopewell, J. W.; Gorlia, T.; Pellettieri, L.; Giusti, V.; Stenham, B. H.; Skold, K. Boron neutron capture therapy for newly diagnosed glioblastoma multiforme: an assessment of clinical potential. *Appl. Radiat. Isot.* **2011**, *69*, 1737–1740.
- (7) Sivaev, I. B.; Bregadze, V. I. Polyhedral boranes for medical applications: current status and perspectives. *Eur. J. Inorg. Chem.* **2009**, *11*, 1433–1450.
- (8) Sibrian-Vazquez, M.; Vicente, M. Boron tumor-delivery for BNCT: recent developments and perspectives. In *Boron Science: New Technologies & Applications*; Hosmane, N. S., Ed.; CRC Press: Boca Raton, FL, 2011; pp 203–232.
- (9) Vicente, M. G. H.; Sibrian-Vazquez, M. Syntheses of boronated porphyrins and their application in BNCT. In *Handbook of Porphyrin Science*; Kadish, K. M., Smith, K. M., Guilard, R., Eds.; World Scientific Publishers: Singapore, 2010; Vol. 4, pp 191–248.
- (10) Bhupathiraju, N. V. S. D. K.; Vicente, M. G. H. Synthesis of carborene-containing porphyrin derivatives for the boron neutron capture therapy (BNCT) of tumors. In *Topics in Heterocyclic Chemistry: Applications of Porphyrinoids*; Paeslesse, R., Ed.; Springer-Verlag: Berlin Heidelberg, 2014; Vol. 2, in press.
- (11) Dougherty, T. J.; Gomer, C. J.; Henderson, B. W.; Jori, G.; Kessel, D.; Korbelik, M.; Moan, J.; Peng, Q. Photodynamic therapy. *J. Nat. Cancer Inst.* **1998**, *90*, 889–905.
- (12) Pandey, R. K. Recent advances in photodynamic therapy. *J. Porphyrins Phthalocyanines* **2000**, *4*, 368–373.
- (13) Brown, S. B.; Brown, E. A.; Walker, I. The present and future role of photodynamic therapy in cancer treatment. *Lancet Oncol.* **2004**, *5*, 497–508.
- (14) Fabris, C.; Vicente, M. G. H.; Hao, E.; Friso, E.; Borsetto, L.; Jori, G.; Miotti, G.; Colautti, P.; Moro, D.; Esposito, J.; Ferretti, A.; Rossi, C. R.; Nitti, D.; Sotti, G.; Soncin, M. Tumour-localizing and -photosensitising properties of meso-tetra(4-nido-carboranylphenyl)-porphyrin (H_2TCP). *J. Photochem. Photobiol., B* **2007**, *89*, 131–138.
- (15) Soncin, M.; Friso, E.; Jori, G.; Hao, E.; Vicente, M. G. H.; Miotti, G.; Colautti, P.; Moro, D.; Esposito, J.; Rosi, G.; Fabris, C. Tumour-localizing and radiosensitising properties of meso-tetra(4-nido-carboranylphenyl)porphyrin (H_2TCP). *J. Porphyrins Phthalocyanines* **2008**, *12*, 866–873.
- (16) Hao, E.; Friso, E.; Miotti, G.; Jori, G.; Soncin, M.; Fabris, C.; Sibrian-Vazquez, M.; Vicente, M. G. H. Synthesis and biological investigations of tetrakis(*p*-carboranylthio-tetrafluorophenyl)chlorin (TPFC). *Org. Biomol. Chem.* **2008**, *6*, 3732–3740.
- (17) Bhupathiraju, N. V. S. D. K.; Vicente, M. G. H. Synthesis and cellular studies of polyamine conjugates of a mercaptomethyl-carboranylporphyrin. *Bioorg. Med. Chem.* **2013**, *21*, 485–495.
- (18) Sibrian-Vazquez, M.; Hao, E.; Jensen, T. J.; Vicente, M. G. H. Enhanced cellular uptake with a cobaltacarborane-porphyrin-HIV-1 Tat 48–60 conjugate. *Bioconjugate Chem.* **2006**, *17*, 928–934.
- (19) Gryshuk, A.; Chen, Y.; Goswami, L. N.; Pandey, S.; Misset, J. R.; Ohlchansky, T.; Potter, W.; Prasad, P. N.; Oseroff, A.; Pandey, R. K. Structure–activity relationship among purpurinimides and bacteriopurpurinimides: trifluoromethyl substituent enhanced the photosensitizing efficacy. *J. Med. Chem.* **2007**, *50*, 1754–1767.
- (20) Ko, Y. J.; Yun, K. J.; Kang, M. S.; Park, J.; Lee, K. T.; Park, S. B.; Shin, J. H. Synthesis and in vitro photodynamic activities of water-soluble fluorinated tetrapyridylporphyrins as tumor photosensitizers. *Bioorg. Med. Chem. Lett.* **2007**, *17*, 2789–2794.
- (21) Samaroo, D.; Vinodu, M.; Chen, X.; Drain, C. M. *meso-Tetra(pentafluorophenyl)porphyrin* as an efficient platform for combinatorial synthesis and the selection of new photodynamic therapeutics using a cancer cell line. *J. Comb. Chem.* **2007**, *9*, 998–1011.
- (22) Miyashita, M.; Miyatake, S.; Imahori, Y.; Yokoyama, K.; Kawabata, S.; Kajimoto, Y.; Shibata, M. A.; Otsuki, Y.; Kirihata, M.; Ono, K.; Kuroiwa, T. Evaluation of fluoride-labeled boronophenylalanine-PET imaging for the study of radiation effects in patients with glioblastomas. *J. Neurooncol.* **2008**, *89*, 239–246.
- (23) Hahn, F.; Schmitz, K.; Balaban, T. S.; Bräse, S.; Schepers, U. Conjugation of spermine facilitates cellular uptake and enhances antitumor and antibiotic properties of highly lipophilic porphyrins. *Chem. Med. Chem.* **2008**, *3*, 1185–1188.
- (24) Garcia, G.; Sarrazy, V.; Sol, V.; Morvan, C. L.; Granet, R.; Alves, S.; Krausz, P. DNA photocleavage by porphyrin–polyamine conjugates. *Bioorg. Med. Chem.* **2009**, *17*, 767–776.
- (25) Sarrazy, V.; Garcia, G.; Bakidi, J. P. M.; Morvan, C. L.; Begaud-Grimaud, G.; Granet, R.; Sol, V.; Krausz, P. Photodynamic effects of porphyrin–polyamine conjugates in human breast cancer and keratinocyte cell lines. *J. Photochem. Photobiol., B* **2011**, *103*, 201–206.
- (26) Sibrian-Vazquez, M.; Jensen, T. J.; Froncsek, F. R.; Hammer, R. P.; Vicente, M. G. H. Synthesis and characterization of positively charged porphyrin–peptide conjugates. *Bioconjugate Chem.* **2005**, *16*, 852–863.
- (27) Sibrian-Vazquez, M.; Nesterova, I. V.; Jensen, T. J.; Vicente, M. G. H. Mitochondria-targeting by guanidine- and biguanidine-porphyrin photosensitizers. *Bioconjugate Chem.* **2008**, *19*, 705–713.
- (28) Chen, X.; Hui, L.; Foster, D. A.; Drain, C. M. Efficient synthesis and photodynamic activity of porphyrin–saccharide conjugates: targeting and incapacitating cancer cells. *Biochemistry* **2004**, *43*, 10918–10929.
- (29) Zheng, X.; Morgan, J.; Pandey, S. K.; Chen, Y.; Tracy, E.; Baumann, H.; Misset, J. R.; Batt, C.; Jackson, J.; Bellnier, D. A.; Henderson, B. W.; Pandey, R. K. Conjugation of HPPH to carbohydrates changes its subcellular distribution and enhances photodynamic activity in vivo. *J. Med. Chem.* **2009**, *52*, 4306–4318.
- (30) Hao, E.; Jensen, T. J.; Vicente, M. G. H. Synthesis of porphyrin–carbohydrate conjugates using “click” chemistry and their preliminary evaluation in human HEp2 cells. *J. Porphyrins Phthalocyanines* **2009**, *13*, 51–59.
- (31) Zhang, M.; Zhang, Z.; Blessington, D.; Li, H.; Busch, T. M.; Madrak, V.; Miles, J.; Chance, B.; Glickson, J. D.; Zheng, G. Pyropheophorbide 2-deoxyglucosamide: a new photosensitizer targeting glucose transporters. *Bioconjugate Chem.* **2003**, *14*, 709–714.
- (32) Deeken, J. F.; Löscher, W. The blood–brain barrier and cancer: transporters, treatment, and trojan horses. *Clin. Cancer Res.* **2007**, *13*, 1663–1674.
- (33) Provenzale, J. M.; Mukundan, S.; Dewhirst, M. The role of blood–brain barrier permeability in brain tumor imaging and therapeutics. *Am. J. Roentgenol.* **2005**, *185*, 763–767.
- (34) Sakurada, S.; Takeda, S.; Sato, T.; Hayashi, T.; Yuki, M.; Kutsuwa, M.; Tan-No, K.; Sakurada, C.; Kisara, K.; Sakurada, T. Role of histamine H₁ receptor in pain perception: a study of the receptor gene knockout mice. *Eur. J. Pharmacol.* **2000**, *395*, 107–112.
- (35) Deguchi, Y.; Miyakawa, Y.; Sakurada, S.; Naito, Y.; Morimoto, K.; Ohtsuki, S.; Hosoya, K.-i.; Terasaki, T. Blood–brain barrier transport of a novel μ 1-specific opioid peptide, H-Tyr-d-Arg-Phe- β -Ala-OH (TAPA). *J. Neurochem.* **2003**, *84*, 1154–1161.
- (36) Mizoguchi, H.; Watanabe, C.; Watanabe, H.; Moriyama, K.; Sato, B.; Ohwada, K.; Yonezawa, A.; Sakurada, T.; Sakurada, S. Involvement of endogenous opioid peptides in the antinociception induced by the novel dermorphin tetrapeptide analog amidino-TAPA. *Eur. J. Pharmacol.* **2007**, *560*, 150–159.
- (37) Ujváry, I.; Nachman, R. J. Synthesis of heterobifunctional *p*-carborane derivatives. 3-[12-(Mercaptomethyl)-1,12-dicarba-closo-dodecaboran(12)-1-yl]propionic acid. *Tetrahedron Lett.* **1999**, *40*, 5147–5149.
- (38) Gaillard, P. J.; de Boer, A. G. Relationship between permeability status of the blood brain barrier and in vitro permeability coefficient of a drug. *Eur. J. Pharm. Sci.* **2000**, *12*, 95–102.
- (39) Grimes, R. N. *Carboranes*, 2nd ed.; Academic Press: Burlington, MA, 2011.
- (40) Allen, F. H. The Cambridge Structural Database: a quarter of a million crystal structures and rising. *Acta Crystallogr.* **2002**, *B58*, 380–388.
- (41) Hao, E.; Froncsek, F. R.; Vicente, M. G. H. Carborane functionalized pyrroles and porphyrins via the Suzuki cross-coupling reaction. *Chem. Commun.* **2006**, 4900–4902.

- (42) Easson, M. W.; Fronczek, F. R.; Jensen, T. J.; Vicente, M. G. H. Synthesis and in vitro properties of trimethylamine- and phosphonate-substituted carboranylporphyrins for application in BNCT. *Bioorg. Med. Chem.* **2008**, *16*, 3191–3208.
- (43) Bhupathiraju, N. V. S. D. K.; Gottumukkala, V.; Hao, H. X.; Fronczek, F. R.; Baker, D. G.; Wakamatsu, N.; Vicente, M. G. H. Synthesis and toxicity of cobalt bisdicarbollide-containing porphyrins of high boron content. *J. Porphyrins Phthalocyanines* **2011**, *15*, 973–983.
- (44) Hao, E.; Jensen, T. J.; Courtney, B. H.; Vicente, M. G. H. Synthesis and cellular studies of porphyrin–cobaltacarborane conjugates. *Bioconjugate Chem.* **2005**, *16*, 1495–1502.
- (45) Hao, E.; Sibrian-Vazquez, M.; Serem, W.; Garno, J. C.; Fronczek, F. R.; Vicente, M. G. H. Synthesis, aggregation and cellular investigations of porphyrin–cobaltacarborane conjugates. *Chem.—Eur. J.* **2007**, *13*, 9035–9042.
- (46) Rothbard, J. B.; Jessop, T. C.; Lewis, R. S.; Murray, B. A.; Wender, P. A. Role of membrane potential and hydrogen bonding in the mechanism of translocation of guanidinium-rich peptides into cells. *J. Am. Chem. Soc.* **2004**, *126*, 9506–9507.
- (47) Weksler, B. B.; Subileau, E. A.; Perrière, N.; Charneau, P.; Holloway, K.; Leveque, M.; Tricoire-Leignel, H.; Nicotra, A.; Bourdoulous, S.; Turowski, P.; Male, D. K.; Roux, F.; Greenwood, J.; Romero, I. A.; Couraud, P. O. Blood–brain barrier-specific properties of a human adult brain endothelial cell line. *FASEB J.* **2005**, *19*, 1872–1874.
- (48) Poller, B.; Gutmann, H.; Krähenbühl, S.; Weksler, B.; Romero, I.; Couraud, P. O.; Tuffin, G.; Drewe, J.; Huwyler, J. The human brain endothelial cell line hCMEC/D3 as a human blood–brain barrier model for drug transport studies. *J. Neurochem.* **2008**, *107*, 1358–1368.
- (49) Markoutsas, E.; Pampalakis, G.; Niarakis, A.; Romero, I. A.; Weksler, B.; Couraud, P.-O.; Antimisiaris, S. G. Uptake and permeability studies of BBB-targeting immunoliposomes using the hCMEC/D3 cell line. *Eur. J. Pharm. Biopharm.* **2011**, *77*, 265–274.
- (50) Bhattacharya, R.; Xu, Y.; Rahman, M. A.; Couraud, P.-O.; Romero, I. A.; Weksler, B. B.; Weidanz, J. A.; Bickel, U. A novel vascular targeting strategy for brain-derived endothelial cells using a TCR mimic antibody. *J. Cell. Phys.* **2010**, *225*, 664–672.
- (51) Van Rooy, I.; Mastrobattista, E.; Storm, G.; Hennink, W. E.; Schiffeler, R. M. Comparison of five different targeting ligands to enhance accumulation of liposomes into the brain. *J. Controlled Release* **2011**, *150*, 30–36.
- (52) Kawabata, S.; Yang, W.; Barth, R. F.; Wu, G.; Huo, T.; Binns, P. J.; Riley, K. J.; Ongayi, O.; Gottumukkala, V.; Vicente, M. G. H. Convection enhanced delivery of carboranylporphyrins for neutron capture therapy of brain tumors. *J. Neurooncol.* **2011**, *103*, 175–185.
- (53) Vandenhoute, E.; Culot, M.; Gosselet, F.; Dehouck, L.; Godfraind, C.; Franck, M.; Plouët, J.; Cecchelli, R.; Dehouck, M.-P.; Ruchoux, M.-M. Brain pericytes from stress-susceptible pigs increase blood-brain barrier permeability in vitro. *Fluids Barriers CNS* **2012**, *9*, 11–22.
- (54) Watson, P. M. D.; Paterson, J. C.; Thom, G.; Ginman, U.; Lundquist, S.; Webster, C. I. Modeling the endothelial blood–CNS barriers: a method for the production of robust in vitro models of the rat blood-brain barrier and blood-spinal cord barrier. *Neuroscience* **2013**, *14*, 59–79.
- (55) Weksler, B.; Romero, I. A.; Couraud, P.-O. The hCMEC/D3 cell line as a model of the human blood brain barrier. *Fluids Barriers CNS* **2013**, *10*, 16–25.
- (56) Faria, A.; Meireles, M.; Fernandes, I.; Santos-Buelga, C.; Gonzalez-Manzano, S.; Dueñas, M.; de Freitas, V.; Mateus, N.; Calhau, C. Flavonoid metabolites transport across a human BBB model. *Food Chem.* **2014**, *149*, 190–196.
- (57) Carl, S. M.; Lindley, D. J.; Couraud, P. O.; Weksler, B. B.; Romero, I.; Mowery, S. A.; Knipp, G. T. ABC and SLC transporter expression and pot substrate characterization across the human CMEC/D3 blood brain barrier cell line. *Mol. Pharmaceutics* **2010**, *7*, 1057–1068.
- (58) Okura, T.; Higuchi, K.; Kitamura, A.; Deguchi, Y. Proton-coupled organic cation antiporter-mediated uptake of apomorphine enantiomers in human brain capillary endothelial cell line hCMEC/D3. *Biol. Pharm. Bull.* **2014**, *37*, 286–291.
- (59) van Rooy, I.; Cakir-Tascioglu, S.; Couraud, P.-O.; Romero, I. A.; Weksler, B.; Storm, G.; Hennink, W. E.; Schiffeler, R. M.; Mastrobattista, E. Identification of peptide ligands for targeting to the blood-brain barrier. *Pharm. Res.* **2010**, *27*, 673–682.